International Journal of Remote Sensing
Vol. 27, No. 23, 10 December 2006, 5253–5268

Delineating lakes and enclosed islands in satellite imagery by geodesic active contour model

C. SHEN*†, J. FAN‡, L. PI§ and F. LI¶

†Joint Laboratory for Imaging Science and Technology and Department of Computer Science, East China Normal University, Shanghai 200062, China

‡Deptartment of Mathematics, East China Normal University, Shanghai 200062, China and School of Mathematics and Information Science, Wenzhou University, Zhejiang 325035, China

§Department of Mathematics, Shanghai Jiao Tong University, Shanghai 200030, China

¶Department of Mathematics, East China Normal University, Shanghai 200062, China

(*Received 22 December 2005; in final form 31 January 2006*)

The objective of the present paper is to develop a new method for delineating lakes and enclosed islands from shuttle radar topography mission (SRTM) digital elevation model (DEM). The Thousand-Island Lake in China is chosen as the study site. DEM may have missing values or be inaccurate over water bodies. Thus, it is not trivial to delineate the shorelines of lake directly from DEM. We achieve this objective by overlaying the boundary derived from the Landsat image of the same area. Unlike traditional water body delineation techniques, e.g. the band ratio method, which make use of physical quantities, we only use the colour information from Landsat ETM+ band 7, 4 and 2. The main reason is that the colour information is the only resource available for most publicly available satellite data such as the maps from Google Earth. Thus, it is necessary to develop a method depending on only colour information. In the Landsat image, a discrimination function to determine whether a pixel belongs to the lake area is obtained by studying sample pixels chosen from the lake area. The delineation of shorelines is an evolutionary process. The evolution equation is derived according to the active contour model and the discrimination function. The initial contour is inside the lake and expands according to the evolution equation. The evolving curve converges to the boundaries of the lake efficiently with a satisfactory result. Finally, the shorelines are overlaid on the DEM according to latitude and longitude. Our geodesic active contour method is a general one, and could be used to delineate objects of interest such as oil slicks and burn scars in satellite images.

1. Introduction

The shuttle radar topography mission (SRTM) is a joint project between the National Geospatial-Intelligence Agency (NGA) and the National Aeronautics and Space Administration (NASA) (Shuttle Radar Topography Mission Homepage). The SRTM digital elevation model (DEM) was calculated from the data acquired by the space shuttle Endeavour in February 2000. DEMs have many useful applications such as watershed delineation and slope map generation for landslide

*Corresponding author. Email: cmshen@cs.ecnu.edu.cn

International Journal of Remote Sensing
ISSN 0143-1161 print/ISSN 1366-5901 online
http://www.tandf.co.uk/journals
DOI: 10.1080/01431160600857444

hazards. In the current paper we develop a method for delineating shorelines of lakes on SRTM DEM, which is useful for applications that need either to keep or to exclude water bodies from DEMs.

It would not be a difficult task to delineate shorelines if the DEM were absolutely accurate. Since a lake surface is flat by definition, all DEM values should be the same or at least similar. Thus, in a DEM map, an area of constant elevation could be easily detected and the boundary of this area would be the shoreline. However, in reality the DEM values are not constant over water bodies because of a limited vertical accuracy (16 m according to NASA). Furthermore, in lake areas, a lot of data are missing because of the mirror effect, and some DEM values could be higher than those of the real lake surface if islands are present within the lake. Therefore, an area of constant elevation corresponding to the lake area rarely exists in the SRTM DEM. Other methods and auxiliary information are required in order to retrieve shorelines.

In the present paper, a Landsat image of the same area is chosen as the auxiliary information. We first retrieve shorelines from the Landsat image using a geodesic active contour model, then overlay the Landsat-retrieved shorelines onto the DEM. The SRTM DEM data are obtained from the U.S. Geological Survey (USGS) (Shuttle Radar Topography Mission Homepage) and have a resolution of three arc seconds (approximately 90 m). The Landsat 7 ETM+ data are obtained from Global Land Cover Facility (GLCF), University of Maryland (Global Land cover Facility Homepage). The Landsat image is displayed in the combination of band 742, i.e. band 7 (2.08–2.35 μm), band 4 (0.76–0.9 μm) and band 2 (0.52–0.6 μm) are shown in red, green and blue (RGB) respectively. The Thousand-Island Lake in Zhejiang Province, China (see figure 1) is chosen as the study site.

The rest of this paper is organized as follows. §2 provides general information on the study area. The corresponding Landsat image and SRTM DEM are presented.

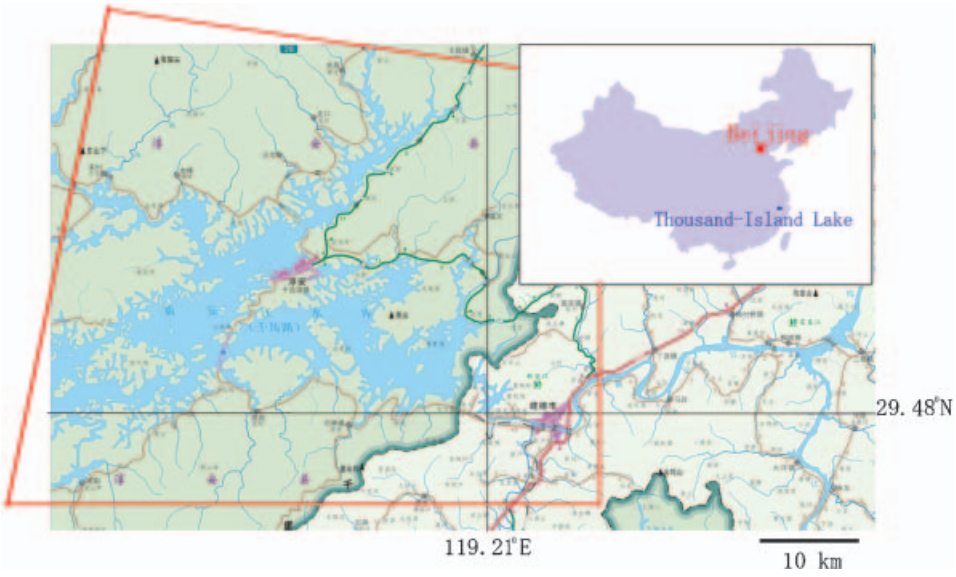

Figure 1. Map of Thousand-Island Lake (light blue indicates the lake; red frame indicates the limit of the Landsat scene shown in figure 3. The intersection of the latitude line and longitude line in the figure is the location of the dam.)

Some of their features are also discussed. §3 is divided into two parts: the first part includes sections 3.1 and 3.2; the second part includes §3.3. §3.1 discusses general active contour models, and demonstrates why they are not applicable to our case. §3.2, the main part of the paper, presents our improved geodesic active contour model. §3.3 describes how to overlay the derived lake boundaries to the DEM. §4 shows the result of the delineated shorelines from the Landsat image and the DEM with the overlaid shorelines. §5 concludes the paper.

2. General information of the study area and corresponding Landsat and DEM images

Our study area is Thousand-Island Lake in Zhejiang Province, China (see figure 1, Hsin-an River Dam 2006). It is a reservoir built mainly in the 1960s, with an area of about 580 km^2. There are 1078 islands (each is larger than 500 m^2) inside the reservoir. The average water level is around 98 m, and the average water depth is 34 m if the water level is at 108 m above sea level. The dam of the reservoir is 465 m long and the top of the dam is at 115 m. The river downstream from the dam is called Xin'an River (in Wade-Giles Spelling System, it is referred as Hsin-an River). Figure 2 shows a photograph of Thousand-Island Lake with some of its islands. The strip of bare, exposed soil (yellow in the figure) is caused by the rising and falling of the water level.

Figure 3 shows the Landsat 7 ETM+ image of Thousand-Island Lake area (combination band 742), and figure 4 shows the SRTM DEM of the same area. The time difference between these two datasets is three months: The DEM was acquired in February 2000, and the Landsat image in May 2000. The water levels at the dates of these two images are not known, but the difference should be small since the period of February to May was not the flood season in this area. The pink pixels between green (vegetation) and blue (water) in figure 3 correspond to the yellow soils in figure 2 because of the difference between the pseudo colour of band 742 and the real colour.

The original DEM (figure 4(a)), compared with figure 3, has a lot of missing data in the lake area. Figure 4(b) shows an interpolation result implemented in the remote sensing software ENVI. Missing data are replaced by values interpolated from valid

Figure 2. Scenery of Thousand-Island Lake.

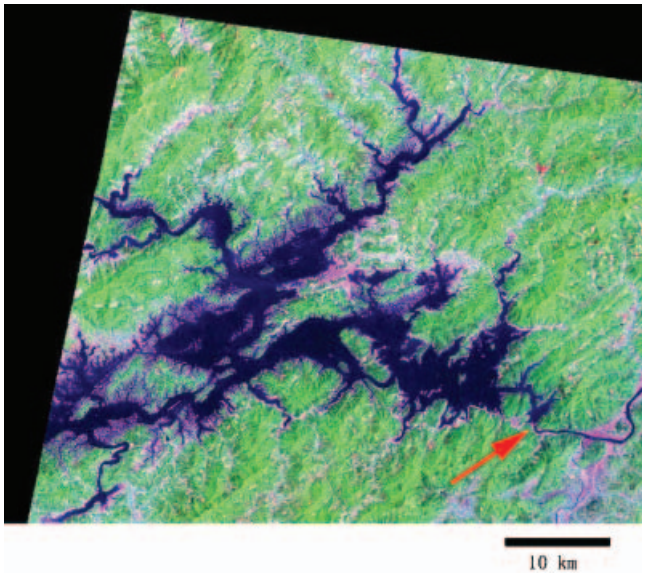

Figure 3. Landsat image of Thousand-Island Lake area, taken on 4 May, 2000. Composite TM bands 7, 4, 2; orbit number: path 119, row 040; red arrow indicates the location of the dam. Courtesy of USGS.

neighboring pixels. It can also be observed that the DEM values of the Xin'an River below the dam are significantly lower than that in the lake area.

The DEM values in the lake area are not constant either in figure 4(a) or figure 4(b), and in certain places the values are obviously wrong. It would be difficult to retrieve shorelines only from these DEMs. Thus our objective is to delineate exterior boundaries (shorelines) and interior boundaries (islands) of Thousand-Island Lake in figure 4(a) or figure 4(b) with the auxiliary information such as figure 3.

Here we shall explain why Landsat 7 image of band 742 combination (band 7 shown as red, band 4 as green, and band 2 as blue) is chosen as the auxiliary information for boundary delineation and why we will not make use of traditional water delineation techniques such as normalized difference water index (NDWI) or band ratio method.

Traditional methods usually use indices such as NDWI or band ratio to distinguish between water and non-water bodies (Huggel *et al.* 2002, McFeeters 1996). However, precise calculations of these indices require a complicated pre-process, such as atmospheric correction, that we wish to avoid. Moreover, since most satellite data that could be used in the retrieval of physical quantities are not free, the choice of auxiliary data is quite limited. Although more and more free data, such as satellite images downloaded from Google Earth, are available, unfortunately, those images (most of them are in JPEG format) only contain colour information. Thus NDWI or band ratio cannot be calculated. Hence, there is a need to develop a water retrieval method from ordinary RGB images which only contain digital number (DN) information in each channel. Here we use Landsat band 742 combination since this combination has an effect similar to natural colours. Each band is a tiff file downloaded from the database of GLCF. Although physical quantities such as radiance could be retrieved from the data, we only use DN

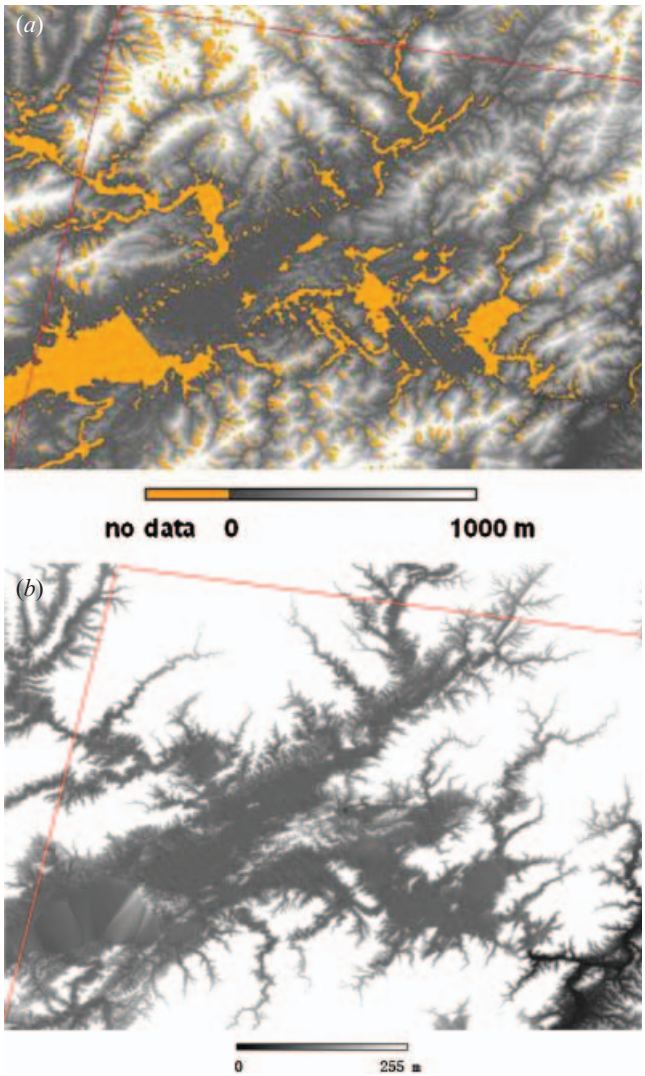

Figure 4. (*a*) DEM of Thousand-Island Lake area with missing values. (Frame indicates the limit of the Landsat scene.) (*b*) DEM data after interpolation (implemented in ENVI).

information, i.e. non-physical information, in our study. Thus, the algorithm developed in the current paper can be transplanted to other DN-based images.

On the other hand, NDWI or band ratio methods also have disadvantages. They require a threshold to be set. A pixel is considered as a water pixel if its index, e.g. NDWI=(TM4−TM1)/(TM4+TM1) is smaller than the threshold. This kind of thresholding criterion is correct at a given probability level and may cause errors. Figure 5 illustrates such an example. Figure 5(a) is a zoom-in of the lower right part of figure 3. Known from the map in figure 1, the reddish points on the north bank of the Xin'an River in figure 5(a) are the urban areas of Jiande City. Figures 5(b) and 5(c) are two thresholding results of NDWI. A point is regarded as a water pixel if NDWI<-0.3 in figure 5(b), and NDWI<-0.5 in figure 5(c). Many urban areas are misclassified as water in figure 5(b) while the criterion is too strict in figure 5(c).

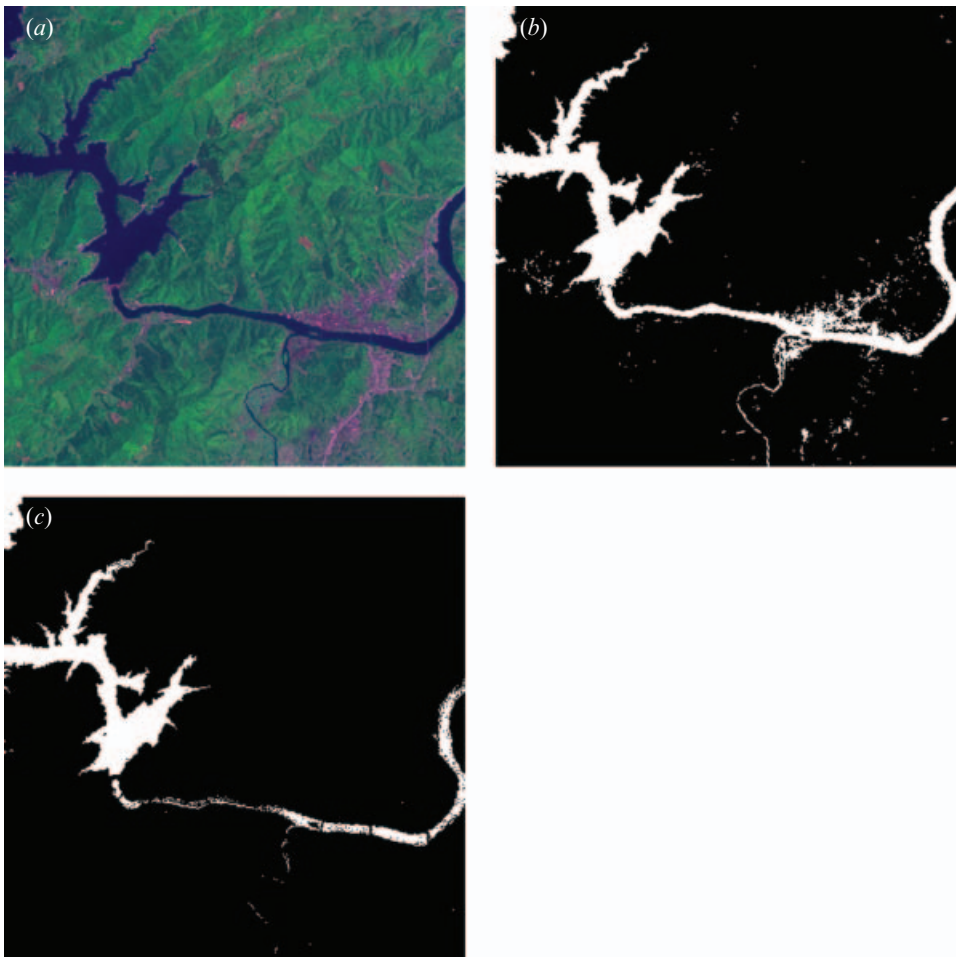

Figure 5. (*a*) Urban area of Jiande City in the Landsat image. (*b*) Thresholding using NDWI<-0.3. (White indicates that the pixel is regarded as a lake pixel.) (*c*) Thresholding using NDWI<-0.5. (White indicates that the pixel is regarded as a lake pixel.)

Thus, a proper threshold should be between -0.5 and -0.3, but it is difficult to get this value accurately.

In addition to the two factors mentioned above, the most important reason is that our method is a general one, and suitable for the boundary delineation not only of water body but also of other objects of interest (OOI). In many cases, even if physical quantities such as NDWI are known, they are not helpful for the delineation. One example is that the burn/fire scar is the OOI. Our method based only on colour information can still be used when the methods depending on physical quantities fail.

3. Delineation of exterior and interior shorelines

We first discuss the mathematical problem concerned in the delineation of exterior and interior shorelines in the Landsat image. Mathematically, our problem is to find a solution on how to delineate the boundaries of OOI.

In general, there are two categories of methods for delineating boundaries of objects: edge detection methods and active contour methods. The first category is not suitable for our case because edge detection methods are threshold-based and thus have two disadvantages: the detected edges may not be continuous and the detected edges may contain many unwanted points. Therefore, we adopt a method from the second category. Our method is a geodesic active contour method developed from the snake algorithm.

3.1 *The snake algorithm and geodesic active contour model*

The snake algorithm is an active contour method to delineate the boundary of objects (Kass *et al.* 1988). Given an initial contour in an image, a corresponding energy can be defined. If the contour changes, the energy will change accordingly. When the energy reaches its minimum, the corresponding contour is regarded as the boundary of object(s).

In our case, the snake algorithm is not applicable as it cannot handle changes in topology. For example, if the initial contour is a circle, no matter how it evolves, it cannot evolve into two circles. Thus, the snake algorithm is only applicable to detecting objects whose topology is the same as that of the initial contour. As we cannot assume that the topology of shoreline will be the same as that of the initial contour, the snake algorithm fails. Besides the problem of topology, the snake algorithm is also not able to detect the interior boundaries of the lake. For example, a given initial contour, e.g. the boundary of the image shrinks during the evolution. The evolution will terminate when the contour reaches the exterior shoreline. Thus, the snake algorithm cannot detect islands. For these two reasons, the snake algorithm is not useful in our case.

The geodesic active contour model is an improved active contour method. It makes use of the concept of the level set method (Osher and Sethian 1988), which can handle topology changes during the evolution. The main idea of the level set method is to regard the evolving contour in the two-dimensional plane as a contour line of an evolving surface in three-dimensional space. Then, the problem of finding the contour is converted to finding the corresponding evolving surface. If the evolving surface is denoted by a family of surfaces $z=\phi(x_1,x_2,t)$, then the evolving contour could be represented by the intersection of $z=\phi(x_1,x_2,t)$ and $z=0$. Here x_1, x_2 are image pixel coordinates, t is the evolution time, and z represents the height of the surface in the location of (x_1,x_2) at time t. If (a) $\phi(x_1,x_2,0)=0$ represents the initial contour, and (b) $\phi(x_1,x_2,t\rightarrow\infty)=0$ tends to the desired contour of objects, then the evolution of contour can be represented by $\phi(x_1,x_2,t)=0$, i.e. $\phi(x_1,x_2,t)=0$ is the implicit representation of the evolving contour in the (x_1,x_2) plane. The evolving level set function $z=\phi(x_1,x_2,t)$ can be obtained by solving its corresponding partial differential equations.

However, even the traditional geodesic active contour model cannot solve our problem directly. The evolving contour may stop at all boundaries it encounters, not only at the shoreline points. In the geodesic active contour model, the evolution speed at every point is controlled by a stopping function defined at that point (Caselles *et al.* 1997). The smaller the stopping function, the smaller the evolution speed. The curve will stop at a point if the evolution speed is reaching zero. Hence a 'wrong' stopping function will cause the evolving contour to stop at wrong places. Unfortunately, a usual stopping function is 'wrong' for our case. It is defined as a decreasing function of the gradient only, i.e. the stopping function is small at the

location where the gradient is large. Thus, the evolving curve may stop at any place where the gradients are large, no matter whether these places are real shorelines or not. Thus the traditional geodesic active contour model does not work unless the stopping function is modified.

The modified stopping function should let the evolving curve stop only at the boundary of OOI, i.e. the boundary of the lake. At other places, the curve should continue marching on no matter how large the gradients are. This requires the characteristics of the lake pixels be studied. In section 3.2, we will show the characteristics of lake pixels by giving a discrimination function derived from analysing their colour information. The discrimination function is used to define a more suitable stopping function.

The other problem of the level set method is the premature termination, which is similar to the problem mentioned for the snake algorithm. Assuming again that the initial curve is the image boundary, it will arrive at the exterior boundary after several successful iterations. Then, we expect it to continue shrinking to reach the interior shoreline (islands). Unfortunately, the iteration terminates when the evolution speed reaches zero at the exterior shoreline. An alternative would be to use the Chan–Vese model (2001). This model can delineate exterior and interior boundaries simultaneously, but is more complicated compared to the geodesic active model using the level set method. In our case, the Chan–Vese model is avoided by expanding the initial contour defined inside the lake. When reaching the interior boundaries (islands) during the expansion, the evolving contour will delineate those islands and go on till the exterior boundary is met.

3.2 *Our algorithm to delineate boundaries of OOI*

In order to delineate interior and exterior shorelines in the Landsat image, we use the following steps.

1. Determine the characteristics of lake pixels using a discrimination function.
2. Set the stopping function for each image pixel.
3. Derive the curve evolution equation.
4. Solve the evolution equation numerically.

In what follows, assume the image $I(x_1,x_2)$ is a colour image of combination band 742 unless stated otherwise. If $x=(x_1,x_2)$, the image can also be expressed by $I(x)$, $I(x)=(I_1(x),I_2(x),I_3(x))=(R,G,B)$.

3.2.1 Discrimination of the lake pixels. In this section, we will study the characteristics of the lake pixels and give a discrimination function to characterize them. The characteristics of the lake pixel population are estimated from samples chosen in the lake. The discrimination function could be expressed in RGB coordinates or other more suitable coordinates in the colour space. Here 'more suitable' means that the expression would be simpler or more precise than in RGB coordinates. The principal component analysis (PCA) is a way to find such 'more suitable' system (Anderson 2003).

The PCA can be briefly explained as follows. In $I(x_1,x_2)$, we choose n sample pixels from the lake, and denote the colour information of the μth sample pixel by $(s_{\mu 1},s_{\mu 2},s_{\mu 3})$, $\mu=1,\ldots,n$. Therefore, $S=(s_{\mu j})$ is an $(n\times 3)$ matrix. Let us express the correlation matrix of S as $C=(c_{ij})_{3\times 3}$. Let $\lambda_1\geqslant\lambda_2\geqslant\lambda_3$ be the eigenvalues of C and $\omega_1,\omega_2,\omega_3$ the corresponding eigenvectors, then these eigenvectors (column vectors)

are the axes of the new coordinate system. The discrimination function will be expressed in this new coordinate system.

Some basic properties of PCA which will be used in this paper are listed below. Suppose a point is (R,G,B) in the RGB coordinate system, then it is $a=(a_1,a_2,a_3)=(\mathrm{R,G,B})\cdot(\omega_1,\omega_2,\omega_3)$ in the new coordinate system. In particular, $(s_{\mu 1},s_{\mu 2},s_{\mu 3})$ in the RGB coordinate system is $(p_{\mu 1},p_{\mu 2},p_{\mu 3})$ in the new coordinate system, where $p_{\mu j}$ is an element in $P=S\cdot(\omega_1,\omega_2,\omega_3)=(p_{\mu j})_{n\times 3}$. Defining $e_i=\dfrac{\lambda_1}{\lambda_1+\lambda_2+\lambda_3}(i=1,2,3)$, if e_1 is large enough, then the first principal component a_1 of a contains most of the information from R, G and B. Roughly speaking, this will keep $100\times e_i\%$ of the original information. In order to keep more information, the second component a_2 may also be taken into consideration.

In what follows, we will construct an interval, called confidence interval, on the ω_1 axis by the method of interval estimation (Anderson 2003). It is constructed by $\left[\overline{P}_1-\dfrac{S_{P_1}}{\sqrt{n}}\cdot t_{\alpha/2},\overline{P}_1+\dfrac{S_{P_1}}{\sqrt{n}}\cdot t_{\alpha/2}\right]$ with the degree of confidence $1-\alpha$ $(0<\alpha<1)$. Here $\overline{P}_1=\dfrac{1}{n}\sum_{\mu=1}^{n}p_{\mu 1}$, $S_{P_1}=\sqrt{\dfrac{1}{n-1}\sum_{\mu=1}^{n}\left(p_{\mu 1}-\overline{P}_1\right)^2}$, and $t_{\frac{\alpha}{2}}$ is the t-value of the t-distribution with n-1 degrees of freedom. α is usually set as $\alpha=0.05$ (i.e. 95% confidence). Similarly, the second interval in ω_2 axis and the third interval in ω_3 axis could be constructed if necessary.

Figure 6 illustrates the new coordinates obtained by PCA and the confidence interval obtained by interval estimation.

Then, for a given pixel x, we could now define a function $\gamma(x)$, which describes whether this point is a lake pixel or not at a given probability level. Supposing that the confidence interval in ω_1 axis is $[a,b]$, and the value of the first principal component is $u(x)$, then the discrimination function $\gamma(x)$ is defined by

$$\gamma(x)=\begin{cases}1 & a\le u(x)\le b,\\ 0 & \text{others.}\end{cases}$$

To be more precise, if the first principal component is in the interval, further judgment can be done: the pixel is regarded as a lake pixel if and only if its first and second principal components are within their respective confidence intervals.

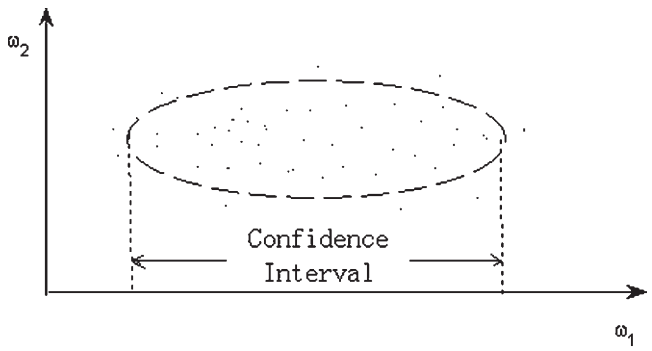

Figure 6. Illustration of PCA and interval estimation.

Figure 7 shows the discrimination result. White indicates that the point is regarded as a lake pixel.

The above PCA, interval estimation and discrimination procedures can be summarized as: Every pixel in the image is transformed from RGB coordinates to the new coordinates via PCA. The pixel is regarded as a lake pixel at a given probability level if its principal component(s) is/are within the confidence interval(s).

Up to this stage, we have actually done something similar to the NDWI method: both methods are threshold-based and may be imprecise at certain points. No matter what method is used, a second step (the modified geodesic active contour model which will be introduced below) will make the result more accurate. Errors in individual points could be (partially) corrected in the evolution. The reason is as follows. During the evolution, the only contribution of the discrimination result is that it helps to construct a stopping function in section 3.2.2. Imprecise discrimination function will cause imprecise stopping function, but the evolution of the curve depends not only on the stopping function. The curve is elastic and a point in the curve is connected with other points like a rubber-band. Thus, for a point with imprecise discrimination value, it is also possible that its neighbouring pixels in the curve will pull the curve to the correct position since the curve has the properties such as regularity.

3.2.2 Stopping function. We shall now define our stopping function by modifying traditional stopping function using the discrimination function.

For a grey image $I(x)$, a stopping function is a decreasing function of the gradient. Usually it only depends on the gradient, regardless of other image information. A typical stopping function is

$$g(x) = \frac{1}{1 + \dfrac{|\nabla(G_\sigma * I)|^2}{K^2}},$$

where $K>0$ is a contrast factor, $G_\sigma(x) = \sigma^{-1/2}\frac{1}{2}\exp\left(-\frac{|x|^2}{4\sigma}\right)$ is a Gaussian filter with a parameter σ, ∇ is the gradient operator, and * is the convolution operator.

A stopping function of such form has disadvantages mentioned in section 3.1. Moreover, it is only applicable to grey images. Here, we define a new stopping

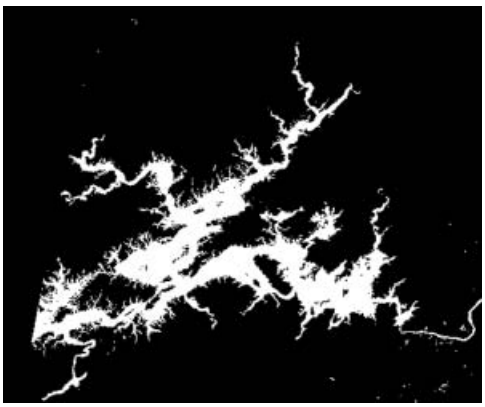

Figure 7. The result of discrimination function. (White indicates that the point is regarded as a lake pixel.)

function for colour images. This stopping function should satisfy: it is small if and only if two conditions are satisfied, i.e. (a) the point is in the lake area, and (b) that point has a large gradient.

In colour images, the concept of gradient is replaced by the largest eigenvalue, denoted by Λ (Sochen *et al.* 1988, Goldenberg *et al.* 2001), of the following matrix

$$\begin{pmatrix} 1+\widetilde{R}_{x_1}^2+\widetilde{G}_{x_1}^2+\widetilde{B}_{x_1}^2 & \widetilde{R}_{x_1}\widetilde{R}_{x_2}+\widetilde{G}_{x_1}\widetilde{G}_{x_2}+\widetilde{B}_{x_1}\widetilde{B}_{x_2} \\ \widetilde{R}_{x_1}\widetilde{R}_{x_2}+\widetilde{G}_{x_1}\widetilde{G}_{x_2}+\widetilde{B}_{x_1}\widetilde{B}_{x_2} & 1+\widetilde{R}_{x_2}^2+\widetilde{G}_{x_2}^2+\widetilde{B}_{x_2}^2 \end{pmatrix},$$

where $\widetilde{R}$, $\widetilde{G}$ and $\widetilde{B}$ represent the pixel's value of R, G and B after Gaussian convolution respectively; $R_{x_i}=\partial_{x_i}R$, etc.

Hence, our stopping function is constructed as

$$g(x)=\frac{1}{1+\gamma(x)\Lambda^2} \tag{1}$$

It can be easily verified that expression (1) satisfies the two conditions mentioned.

3.2.3 Evolution equation. Let $\overrightarrow{C}_t$ be the evolving curve at time t, i.e. $\phi(x,t)=0$ be the implicit representation of $\overrightarrow{C}_t$. For our model in its level set formulation, the partial differential equation of $\phi(x,t)$ should satisfy (Kühne *et al.* 2002, Pi *et al.* 2006):

$$\begin{cases} \frac{\partial\phi}{\partial t}=|\nabla\phi|\mathrm{div}\left(g(x)\dfrac{\nabla\phi}{|\nabla\phi|}\right)+v\cdot g(x)|\nabla\phi|, \\ \phi(x,0)=\phi_0(x), \end{cases} \tag{2}$$

where v is a constant called balloon force, and $\phi_0(x)$ is the level set function for the initial curve, i.e. $\phi_0(x)=0$ is the initial curve. The balloon force indicates whether the contour will shrink or expand. Here it is set as $v<0$, meaning that the contour will expand. The initial curve can be any closed curve or several closed curves inside the lake. Choosing several closed curves at different places will accelerate the speed of evolution.

3.2.4 Numerical solution of the evolution equation. In order to solve equation (2) numerically, the additive operator splitting (AOS) numerical method is used. The AOS scheme is an unconditionally stable numerical scheme for nonlinear diffusion in image processing (Kühne *et al.* 2002). The iterated formula of equation (2) is

$$\phi^{k+1}=\frac{1}{2}\sum_{l=\{x_1,x_2\}}\left[E-2\tau A_l\left(\phi^k\right)\right]^{-1}\left(\phi^k+\tau v g(x)\right),$$

where τ is the time step, E is an identity matrix, and $A_l(\phi^k)$ is a matrix corresponding to the derivatives along the l-th coordinate axis (Kühne *et al.* 2002).

In this iteration scheme, the difference between ϕ^{n+1} and ϕ^n is compared. The evolution will terminate if the difference is less than certain predetermined value. Then, $\phi(x_1,x_2)$ is denoted as the iterated result of ϕ^n.

The exact solutions $\{(x_1,x_2)\}$ of $\phi(x_1,x_2)=0$ would not normally be integer-valued. However, the integer solutions of $\phi(x_1,x_2)=0$ is required owing to the discreteness of grid points. The integer solution can be found by comparing every pixel (x_1,x_2) with its eight-neighbourhood pixels. Define $\mathrm{sign}(x_1,x_2)=\begin{cases} 1 & \text{if } \phi(x_1,x_2)\geq 0 \\ -1 & \text{else} \end{cases}$, then

(x_1,x_2) is regarded as the solution of $\phi(x_1,x_2)=0$ if and only if

$$8\cdot\mathrm{sign}(x_1,x_2)-\sum_{(y_1,y_2)\in 8-\text{neighbour of }(x_1,x_2)}\mathrm{sign}(y_1,y_2)>0$$

i.e. the sign of $\phi(x_1,x_2)$ changes in the eight-neighbourhood of (x_1,x_2).

Thus, the contour $\phi(x_1,x_2)=0$ is found. This contour is the exterior and interior boundaries of the lake.

For the detailed mathematical description for our algorithm of modified geodesic active contour model, please refer to (Pi *et al.* 2006).

3.3 *Overlaying delineated shorelines to DEM*

The latitude/longitude of every pixel in the delineated shorelines is known since the Landsat image has geographical information. Therefore the delineated shorelines can be overlaid to the registered DEM according to latitude/longitude.

4. Results

Figure 8 shows the delineation result in the Landsat image. Seven pixels were chosen as sample points from various locations of the lake and the borders between the lake and islands (see figure 9). The discrimination function is obtained by doing interval estimations along ω_1 and ω_2 axes. The parameters for evolution are: iteration = 450, $\tau=3$, $v=-0.3$, $\sigma=0.5$.

The result is compared with that by NDWI (see figure 10). Figure 10 is obtained by using the threshold NDWI<-0.4. It is hard to judge which one is more accurate since there is no ground truth. The results are similar by visual inspection. The contour expands during the evolution and stops exactly at the location of shorelines in the Landsat image. This could be verified by the fact that the contour is stopped at the location of the dam (see figure 11).

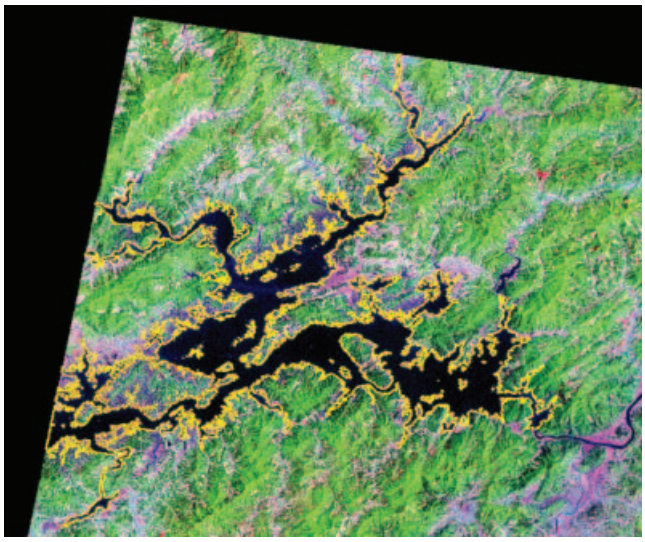

Figure 8. Delineated interior and exterior boundaries (shown in yellow) obtained by the geodesic active contour model.

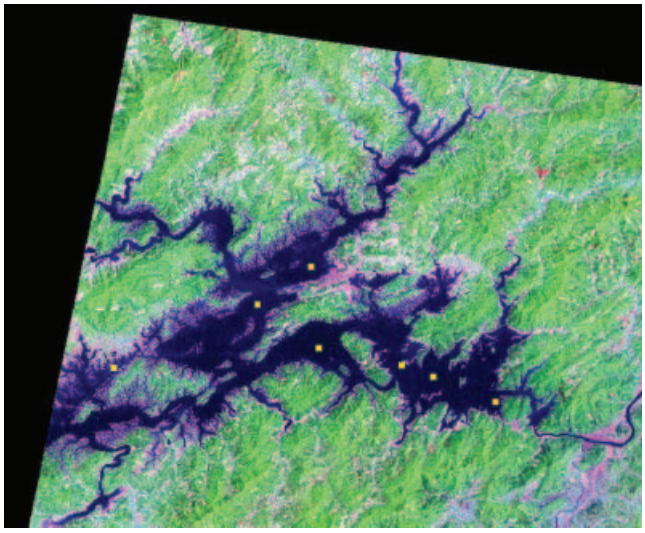

Figure 9. A map showing the sample points in the lake.

Figure 12 shows the delineation result overlaid to the registered SRTM DEM. The accuracy of the overlaid contour could be verified by the fact that the contour just coincides with the location of the dam in the DEM map.

5. Conclusion

We have proposed a method for delineating shorelines from satellite images. The Thousand-Island Lake in China was chosen as the study area. First, the interior and exterior shorelines of the lake are delineated from the Landsat data via the method of modified geodesic contour model. Then the shorelines are overlaid to the registered DEM according to latitude/longitude. The SRTM DEM with overlaid

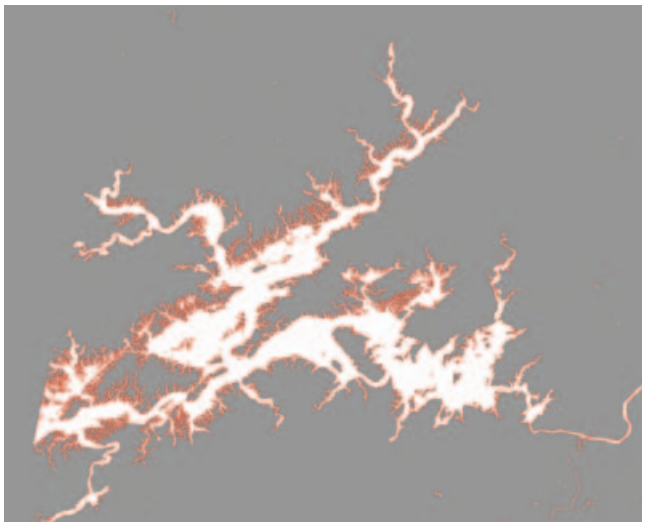

Figure 10. Result of threshold using NDWI<-0.4. (White indicates that the point is regarded as a lake pixel. Brown indicates the boundaries of the lake).

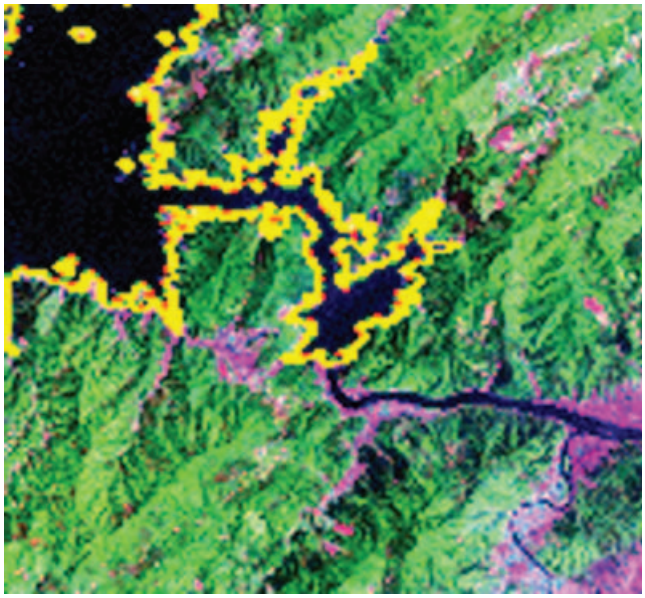

Figure 11. A close look of the delineation result near the location of the dam (zoom-in of the dam area in figure 8).

shorelines could be a value-added product for both researchers who want to study or exclude water bodies.

The main part of this paper describes the algorithm to delineate interior and exterior boundaries of the lake. The major novelty of this paper is that our algorithm can do the water body delineation for ordinary colour images which only contain DN information, avoiding the retrieval of physical quantities such as NDWI. Other improvements include a specific stopping function for lake pixels.

However, this geodesic active contour method also has its shortcomings. First, it cannot delineate interior boundaries when shrinking, although we have avoided this

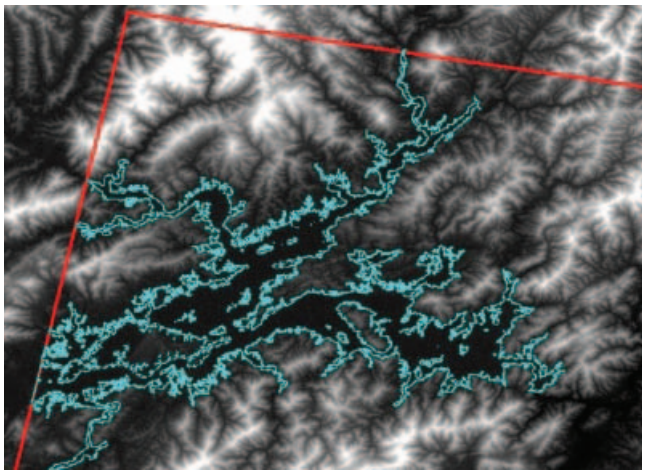

Figure 12. Thousand-Island Lake DEM with overlaid Landsat-delineated shorelines.

difficulty by choosing the method of expansion. A solution for this problem is the Chan–Vese model (2001). Second, the method for the construction of discrimination function is only applicable to the OOI with relatively uniform RGB values. In our case, this shortcoming is not obvious since the water body of Thousand-Island Lake is quite uniform. For less-uniform OOI, the discrimination method could be improved by regarding a less-uniform OOI as several relatively uniform sub-OOIs, then same techniques be applied to these sub-OOIs, and finally combining the results.

To conclude, our geodesic active contour method is a general method for the boundary delineation not only of water bodies but also of other OOI. Similar methods may be applied to solve problems such as the delineation of oil slicks on sea surface or the delineation of burn scars (Shen *et al.* 2005).

Acknowledgements

This research is supported by the National Science Foundation of China (No. 10371039). The authors would like to thank US Geological Survey (USGS) for providing the SRTM DEM data, and Global Land Cover Facility (GLCF), University of Maryland for providing the Landsat imagery. The authors also would like to thank Christian Melsheimer and Lee Ken Yoong for discussion. The authors are grateful to anonymous referees for helpful suggestions.

References

ANDERSON, T.W., 2003, *An Introduction to Multivariate Statistical Analysis*, 3rd edition (New York: John Wiley).

CASELLES, V., KIMMEL, R. and SAPIRO, G., 1997, Geodesic active contours. *International Journal of Computer Vision*, **22**, pp. 61–79.

CHAN, T. and VESE, L., 2001, Active contour without edges. *IEEE Transactions on Image Processing*, **10**, pp. 266–277.

GLOBAL LAND COVER FACILITY HOMEPAGE. http://glcf.umiacs.umd.edu/index.shtml

GOLDENBERG, R., KIMMEL, R., RIVLIN, E. and RUDZSKY, M., 2001, Fast geodesic active contours. *IEEE Transactions on Image Processing*, **10**, pp. 1467–1475.

HSIN-AN RIVER DAM, 2006, *Encyclopædia Britannica*, Encyclopædia Britannica Premium Service, http://www.britannica.com/eb/article-9041292 (accessed 3 February 2006).

HUGGEL, C., KÄÄB, A., HAEBERLI, W. and PAUL, F., 2002, Remote sensing based assessment of hazards from glacier lake outbursts: a case study in the Swiss Alps. *Canadian Geotechnical Journal*, **39**, pp. 316–330.

KASS, M., WITKIN, A. and TERZOPOULOS, D., 1988, Snakes: active contour models. *International Journal of Computer Vision*, **1**, pp. 321–331.

KÜHNE, G., WEICKERT, J., BEIER, M. and EFFELSBERG, W., 2002, Fast implicit active contour models. In *The German Association for Pattern Recognition (Deutsche Arbeitsgemeinschaft für Mustererkennung eV, DAGM) 2002, Lecture Notes in Computer Science*, **2449**, pp. 133–140.

MCFEETERS, S.K., 1996, The use of normalized difference water index (NDWI) in the delineation of open water features. *International Journal of Remote Sensing*, **17**, pp. 1425–1432.

OSHER, S. and SETHIAN, J.A., 1988, Fronts propagating with curvature-dependent speed: Algorithms based on Hamilton–Jacobi formulations. *Journal of Computational Physics*, **79**, pp. 12–49.

PI, L., FAN, J.S. and SHEN, C.M., 2006, Segmentation for objects of interest with modified geodesic active contour. *Journal of Mathematical Imaging and Vision*, in press.

SHEN, C.M., PI, L., LI, F. and FAN, J.S., 2005, Burn scar delineation from Landsat imagery using modified Chan-Vese model. In *Proceedings of the 26th Asian Conference on Remote Sensing*, 7–11 Nov 2005, Hanoi, Viet Nam. CD-ROM.

SHUTTLE RADAR TOPOGRAPHY MISSION HOMEPAGE. Available at: http://srtm.usgs.gov

SOCHEN, N., KIMMEL, R. and MALLADI, R., 1988, A general framework for low level vision. *IEEE Transactions on Image Processing*, **7**, pp. 310–318.